

Improving SUSY Spectrum Determinations at the LHC with the Wedgebox Technique

Ran Lu^a Mike Bisset^b Nick Kersting^c

^a*Department of Physics, University of Michigan*

^b*Department of Physics, Tsinghua University, P.R. China*

^c*Physics Department, Sichuan University, P.R. China*

E-mail: luran@umich.edu, bisset@mail.tsinghua.edu.cn,
nkersting@scu.edu.cn

ABSTRACT: The LHC has the potential not only to discover supersymmetry (SUSY), but also to permit fairly precise measurements of at least a portion of the sparticle spectrum. Proposed mass reconstruction methods rely upon either inverting invariant mass endpoint expressions or upon solving systems of mass-shell equations. These methodologies suffer from the weakness that one certain specific sparticle decay chain is assumed to account for all the events in the sample. Taking two examples of techniques utilizing mass-shell equations, it is found that also applying the wedgebox technique allows for the isolation of a purer event sample, thus avoiding errors, possibly catastrophic, due to mistaken assumptions about the decay chains involved and simultaneously improving accuracy. What is innovative is using endpoint measurements (via the wedgebox technique) to obtain a more homogeneous, well-understood sample set rather than just using said endpoints to constrain the values of the masses (here found by the mass-shell technique). The fusion of different established techniques in this manner represents a highly profitable option for LHC experimentalists who will soon have data to analyze.

KEYWORDS: Supersymmetry, sparticles, mass measurements, wedgebox technique

ARXIV EPRINT: [0806.2492](https://arxiv.org/abs/0806.2492)

Contents

1	Introduction	1
2	The N-MST Method of Nojiri <i>et al.</i>	3
2.1	Addition of the Wedgebox Technique	4
2.1.1	Box Topology	4
2.1.2	Wedge Topology	5
3	The C-MST Method of Cheng <i>et al.</i>	8
3.1	Wedgebox selection	10
4	Discussion & Conclusions	14
5	Acknowledgements	18

1 Introduction

LHC experimentalists will soon determine whether or not Supersymmetry (SUSY) is a TeV-scale phenomenon: if so, colored sparticles will probably be the first to be discerned, possibly soon followed by neutralinos, charginos, and sleptons if favorable decay channels are open, though measuring the masses of these latter colorless sparticles with percent precision will be challenging[1, 2]. The reason for this is that every R-parity-conserving¹ SUSY event produces at least two invisible particles (the lightest SUSY particles, or LSPs) which carry away significant missing energy and make it impossible to reconstruct mass peaks. Therefore, many SUSY mass extraction techniques depend on precise measurement of invariant mass distribution endpoints. For a sparticle decaying into an LSP and a Standard Model (SM) fermion pair, either via a three-body decay or sequential two-body decays, it is straight-forward to see how the endpoint of the di-fermion invariant mass distribution yields the mass difference between the decaying sparticle and the LSP (perhaps modified by the on-mass-shell intermediate for two-body decays) [4–9]. Studies attempting to fully reconstruct the actual sparticle masses from invariant mass endpoint information rely on *specific* longer decay chains, typically $\tilde{q} \rightarrow \tilde{\chi}_2^0 q \rightarrow \tilde{\ell}^\pm \ell^\mp q \rightarrow \tilde{\chi}_1^0 \ell^+ \ell^- q$ [10–24] — each event would have two \tilde{q} ’s (for instance) produced. It is then theoretically doable to construct enough invariant mass distributions to determine the sparticle masses; however, in practice endpoint measurement may be complicated by low event rates, fitting criteria, unaccounted-for (in the simulation) higher-order and radiative[25] effects, and (in particular) backgrounds.

¹If R-parity is not conserved, then it may be possible to fully reconstruct events. See [3] for further details.

Ideas on how to measure SUSY masses without relying on distribution endpoints have also been put forward. The work of Nojiri *et al.*[26, 27], for example, uses mass-shell relations in a sufficiently long SUSY decay chain, *e.g.* $\tilde{g} \rightarrow b \tilde{b} \rightarrow \tilde{\chi}_2^0 bb \rightarrow \tilde{l}^\pm l^\mp bb \rightarrow l^\pm l^\mp bb \tilde{\chi}_1^0$; if some of the masses are already known in this chain the others can *in principle* be found by solving mass-shell relations for a small sample of events², which may in fact lie far from the endpoint. Another method, due to Cheng *et al.*[28–30], starts from very similar looking mass-shell relations, but instead of assuming some masses and solving for the others, scans the whole mass-space for points where these relations are most likely to be satisfied. Both methods, hereafter designated as ‘Mass Shell Techniques’ (MSTs)³, seem quite effective in obtaining percent-level determination of the sought-after SUSY masses, at least at the parameter points considered in those works.

The accuracy of both these MSTs hinges on one critical assumption: the decay topology of choice has been isolated. In the actual LHC data, the decay topology would have to be inferred, if this is at all possible, before proceeding; MSTs would thus appear to be excellent roads to SUSY mass reconstruction which, however, begin only at a point half-way to the destination.

The present work focuses on the first half of this road; *i.e.*, isolating a desired decay topology, and on how this affects a subsequent MST analysis. As a first foray into this potentially quite thorny task, let’s restrict ourselves to just the specific topologies considered in [26] and [28–30] involving a pair of neutralinos $\tilde{\chi}_i^0 \tilde{\chi}_j^0$ ($i, j = 2, 3, 4$) that subsequently decay to leptons (electrons and muons) via on-shell sleptons. This situation is amenable to a wedgebox analysis [32, 33] which is based upon a scatter plot of the di-electron mass $M_{e^+e^-}$ versus the dimuon mass $M_{\mu^+\mu^-}$. A key benefit of this technique is that it allows (at least partial) separation of individual events according to the specific (i, j) -pair whose production gave rise to them. Given sufficient statistics, events from each such decay-type fall in distinct, easily-recognized zones of the wedgebox plot. The overall topology of the resulting wedgebox plot then tests for the significant presence of the various possible (i, j) decay channels — which may for instance signal the meaningful presence of a decay channel erroneously assumed to have been insignificant as the basis for a MST analysis. Events can be selected from a specific zone of the wedgebox plot, preferably a zone populated by only one decay channel. This acts to maximize sample homogeneity and assure the basic MST assumption is satisfied.

Although the wedgebox technique relies on locating the endpoints of invariant mass distributions — just like the studies [10–24] mentioned earlier, the information sought is radically different: the wedgebox analysis is tailor-made for event sample sets comprised of assorted produced sparticle pairs and multiple sparticle decay chains. The observed endpoints serve to delineate the zones and allow for selection of purer subset(s) from an overall sample set. (Using this endpoint information to determine a set of cuts is a far more rational course than that of arbitrarily choosing some numerical cut-off values to purify the data sample.) Virtually all previous studies *presume* such purification has already been accomplished either by an unspecified set of cuts or a fortuitous choice of SUSY input

²In practice, many events are still required.

³Refs. [26, 27, 31] use the name ‘mass relation method’ to refer to their technique.

parameters. The wedgebox technique illustrates a concrete method of how to deal with the more general case, and the consequences which result and should not be ignored in a coupled analysis aiming to extract the sparticle masses.

This paper will show that MSTs, by construction unrelated to invariant mass endpoints, can nevertheless be improved by information contained in these endpoints — specifically via the wedgebox technique⁴. The paper is organized as follows: Sections 2 and 3 concentrate on the ‘N-MST’ method of Nojiri *et al.* and the ‘C-MST’ method of Cheng *et al.*, respectively; Section 4 then offers conclusions and some additional discussion on SUSY mass spectral analyses at the LHC.

2 The N-MST Method of Nojiri *et al.*

For the N-MST method, the focus will be on the decay of a heavy MSSM pseudoscalar Higgs boson as considered in [26]. The specific decay chain is

$$pp \rightarrow A^0 \rightarrow \tilde{\chi}_i^0 \tilde{\chi}_j^0 \rightarrow \tilde{l}_1^\pm l_1^\mp \tilde{l}_2^\pm l_2^\mp \rightarrow l_1^\mp l_1'^\pm l_2^\mp l_2'^\pm \tilde{\chi}_1^0 \tilde{\chi}_1^0 \quad (2.1)$$

where the Higgs boson decays to neutralinos ($i, j = 2, 3, 4$) via on-shell sleptons of the electron- or muon- variety (see Fig. 1). Assuming the final leptons’ four-momenta are

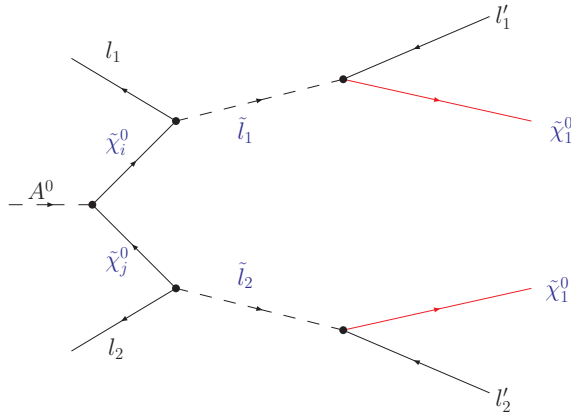


Figure 1. Feynman diagram for the decay (2.1). Here $i, j = 2, 3, 4$ while the label 1 or 2 on leptons stands for either e or μ .

known while the LSP’s escape detection, (2.1) implies six mass-shell constraints on the

⁴Though our strategy is quite different from the ‘hybrid’ method of [31] which couples an MST with values for of endpoints.

eight unknown components of LSP four-momenta (p^μ and p'^μ),

$$m_{\widetilde{\chi}_1^0}^2 = p^2 \quad (2.2)$$

$$m_{\widetilde{\chi}_1^0}^2 = p'^2 \quad (2.3)$$

$$m_{\widetilde{l}_1}^2 = (p_{l_1} + p)^2 \quad (2.4)$$

$$m_{\widetilde{l}_2}^2 = (p_{l_2} + p')^2 \quad (2.5)$$

$$m_{\widetilde{\chi}_i^0}^2 = (p_{l_1} + p'_{l_1} + p)^2 \quad (2.6)$$

$$m_{\widetilde{\chi}_j^0}^2 = (p_{l_2} + p'_{l_2} + p')^2 \quad (2.7)$$

Nojiri *et al.* also posit two overall momentum conservation constraints

$$(p_{l_1} + p_{l_2} + p'_{l_1} + p'_{l_2} + p + p') \cdot \vec{x} = 0 \quad (2.8)$$

$$(p_{l_1} + p_{l_2} + p'_{l_1} + p'_{l_2} + p + p') \cdot \vec{y} = 0 \quad (2.9)$$

along directions (x , y) transverse to the beam (the z -direction), though this would appear to be contingent on the Higgs boson having no transverse momentum. If all the masses $m_{\widetilde{\chi}_1^0}$, $m_{\widetilde{l}_1}$, $m_{\widetilde{l}_2}$, $m_{\widetilde{\chi}_i^0}$, and $m_{\widetilde{\chi}_j^0}$ are known in advance, one can solve the eight equations (2.2)-(2.9) for the eight unknowns and reconstruct the Higgs boson mass via

$$m_A^2 = (p_{l_1} + p_{l_2} + p'_{l_1} + p'_{l_2} + p + p')^2 \quad (2.10)$$

from just one Higgs boson event of the type (2.1). However, even in this idealized scenario which does not include detector resolution, particle widths, backgrounds, *etc.*, there are two major caveats which prevent this procedure from being so straightforward:

- There is a 4-fold ambiguity in assigning labels $l_{1,2}, l'_{1,2}$ to the leptons; this forms a combinatoric background.
- Combining (2.2)-(2.9) leads to a quartic equation with 0, 2 or 4 solutions for the unknown momenta.

So what one must do in practice is collect a number of events and deduce the correct value of m_A from the maximum of the resulting distribution. In [26] a 10^3 event sample (with no backgrounds) thus yielded a percent-level determination of the Higgs boson mass.

2.1 Addition of the Wedgebox Technique

2.1.1 Box Topology

As shown in [26] the programme sketched in the previous section works fairly well at Snowmass Benchmark SPS1a [34] where the dominant Higgs boson decays are via (2.1) with $i = j = 2$. Therein, 1000 events of the type $A^0 \rightarrow \widetilde{\chi}_2^0 \widetilde{\chi}_2^0 \rightarrow llll \widetilde{\chi}_1^0 \widetilde{\chi}_1^0$ were generated using the HERWIG6.4 [35–37] event generator and passed through the detector simulator package ATLFEST [38]. The only cuts required were that all four *isolated* leptons have $\eta < 2.5$, with two of the leptons also having $p_T > 20 \text{ GeV}$ while the other two have $p_T > 10 \text{ GeV}$. Same-flavor events such as $e^+e^-e^+e^-$ or $\mu^+\mu^-\mu^+\mu^-$ were also included

if one of the two possible pairings of OS leptons in such configurations gave a di-lepton invariant mass beyond the ~ 78 GeV kinematic endpoint (implying the other possible pairing is the correct one). This analysis yielded the correct Higgs boson mass with a resolution of only 6 GeV [26].

The following set of cuts are herein adopted in a effort to reproduce these results using ISAJET[39, 40] in place of HERWIG:

1. Leptons must be *hard* ($p_T^\ell > 10, 8$ GeV for e^\pm, μ^\pm , respectively; $|\eta^\ell| < 2.4$), and *isolated* (no tracks of other charged particles in a $r = 0.3$ rad cone around the lepton, and less than 3 GeV of energy deposited into the electromagnetic calorimeter for $0.05 \text{ rad} < r < 0.3 \text{ rad}$ around the lepton).
2. There must be missing energy in the range: $20 \text{ GeV} < E_T < 130 \text{ GeV}$.
3. No jets⁵ are present with a reconstructed energy E_{jet} greater than 50 GeV.

A sufficient sample of $pp \rightarrow A^0$ events is collected to represent an integrated LHC luminosity of 300 fb^{-1} . With this stricter set of cuts it should be somewhat harder to extract the Higgs boson mass.

Fig. 2a shows the wedgebox plot at SPS1a for $e^+e^-\mu^+\mu^-$ events. A ‘simple box’ topology consistent with the expected $\tilde{\chi}_2^0\tilde{\chi}_2^0$ origin of lepton pairs is clear. Moreover, the number of flavor-balanced events ($e^+e^-e^+e^- + \mu^+\mu^-\mu^+\mu^- + e^+e^-\mu^+\mu^-$) exceeds the number of flavor-unbalanced events ($e^+e^-e^\pm\mu^\mp + \mu^+\mu^-\mu^\pm e^\mp$) at this parameter point [41]; this indicates that the events come primarily from a Higgs boson decay⁶ with decay topology (2.1). Though the final number of events passing cuts is somewhat small (only 30 or so compared to the 1000 which [26] assumes, mainly due to the inclusion of the leptonic branching ratios) the number of events in the distribution of solutions is quite a bit larger: recall the bulleted caveats earlier which potentially can yield a $4 \times 4 = 16$ -fold multiplicity factor. Though only a factor of 4 or so is observed, nonetheless a fairly clear peak in the distribution emerges (see Fig. 2b) at the correct value⁷ of $m_A = 400 \pm 5$ GeV.

2.1.2 Wedge Topology

In principle, this method should work for the case $i \neq j$ as well; to test this we consider the following MSSM parameter point:

MSSM Test Point I

$$\begin{aligned} \mu &= 190 \text{ GeV} & M_2 &= 280 \text{ GeV} & \tan \beta &= 10 & M_A &= 600 \text{ GeV} \\ M_{\tilde{e}, \tilde{\mu}_{L,R}} &= 150 \text{ GeV} & M_{\tilde{\tau}_{L,R}} &= 250 \text{ GeV} & M_{\tilde{q}, \tilde{g}} &= 1000 \text{ GeV}. \end{aligned}$$

which has the mass spectrum shown in Table 1. Now the main production modes con-

⁵Jets are defined by a cone algorithm with $r = 0.4$ and must have $|\eta_j| < 2.4$.

⁶Note that though in a simulation one can of course choose to only generate Higgs boson decay events, experimentalists lack this freedom.

⁷Also note here that the momentum-conservation constraints (2.9) do not appear to be generally true; *i.e.*, according to this analysis the parent Higgs boson is often generated with significant transverse momentum in the range $0 \lesssim p_T \lesssim 100$ GeV. Surprisingly, this does not seem to affect the result.

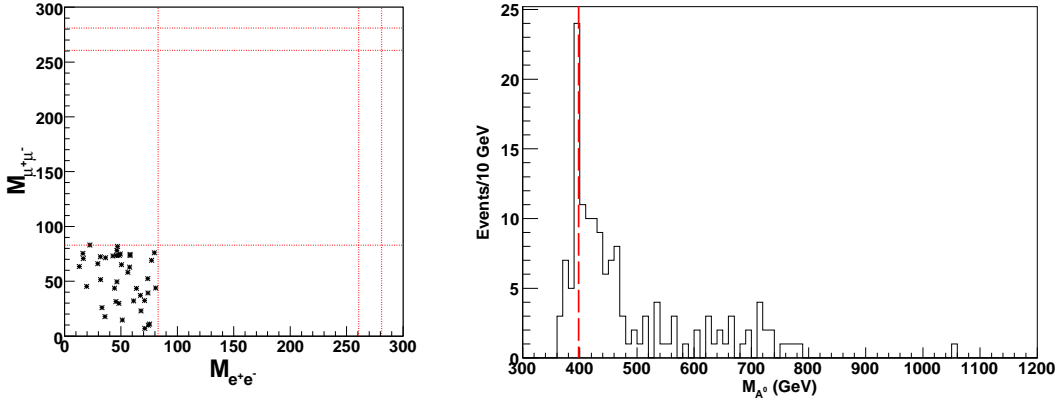


Figure 2. (a) Wedgebox plot at SPS1a (A^0 bosons only) for 300 fb^{-1} luminosity, cuts as in text. Dotted lines show locations of kinematic endpoints from $\tilde{\chi}_{2,3,4}^0 \rightarrow \tilde{\chi}_1^0$ decays. (b) Distribution of solutions for SPS1a. Here the maximum is at the correct Higgs boson mass of $M_A \approx 395$ GeV.

Table 1. Relevant masses at the MSSM Test Point I,II

Particle	Mass (Point I) (GeV)	Mass (Point II) (Gev)
$\tilde{\chi}_1^0$	119.94	86.03
$\tilde{\chi}_2^0$	180.33	143.09
$\tilde{\chi}_3^0$	197.98	166.40
$\tilde{\chi}_4^0$	317.72	277.27
\tilde{e}_R	156.17	127.20
$\tilde{\mu}_R$	156.17	127.20
A^0	600.0	700.00
H^0	609.28	705.58

tributing to the $e^+e^-\mu^+\mu^-$ signal are the Higgs boson channels $H^0/A^0 \rightarrow \tilde{\chi}_2^0\tilde{\chi}_2^0, \tilde{\chi}_2^0\tilde{\chi}_3^0, \tilde{\chi}_2^0\tilde{\chi}_4^0$, ‘direct’ neutralino pair production channels⁸ $\tilde{\chi}_2^0\tilde{\chi}_3^0$ & $\tilde{\chi}_2^0\tilde{\chi}_4^0$, and ‘mixed’ channels involving charginos, mainly $\tilde{\chi}_2^\pm\tilde{\chi}_2^\mp$ & $\tilde{\chi}_2^\pm\tilde{\chi}_{2,3,4}^0$ production. A random sample of $e^+e^-\mu^+\mu^-$ events⁹ will therefore not be a clean collection of Higgs boson decays, which for the luminosity considered here (300 fb^{-1}) number about 150 against nearly 800 direct channel and 100 or so mixed channel events. This point then presents a more challenging case for applying the mass relation method.

However, the shape of the wedgebox plot at this point suggests selecting events via their decay topology: Fig. 3a shows a clear ‘double wedge’ topology implying that events due to $\tilde{\chi}_2^0\tilde{\chi}_2^0$ decays are confined to the innermost box bounded by kinematic edges at ~ 60 GeV,

⁸As explained in [33], direct $\tilde{\chi}_2^0\tilde{\chi}_2^0$ channels are suppressed by isospin symmetry, while $\tilde{\chi}_{3,4}^0\tilde{\chi}_{3,4}^0$ are phase-space suppressed.

⁹Note that for **MSSM Test Point I** the staus have been set more massive than the other sleptons to avoid tau-containing decays and generate more decays to the desired leptons. This is simply done by hand here for convenience.

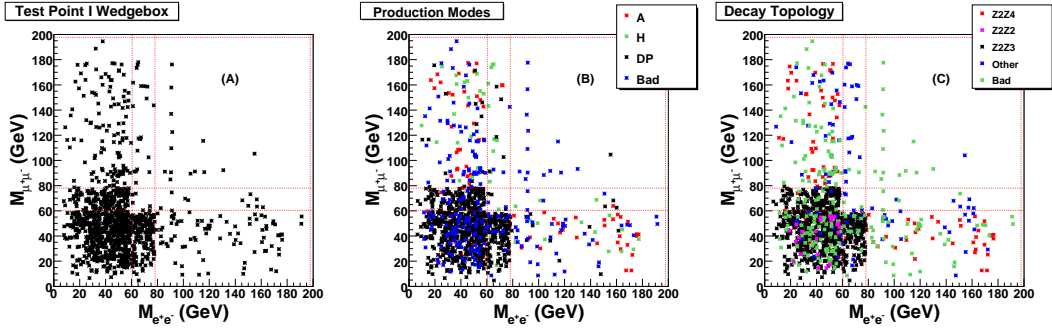


Figure 3. (A) Wedgebox plot for the MSSM Test Point I defined in the text, for 300 fb^{-1} . (B) origin of each four lepton event labeled as from ‘A’, ‘H’, ‘DP’(direct production), or otherwise ‘Bad’. (C) specific pair of neutralinos decaying to each four lepton event identified as $\tilde{\chi}_2^0\tilde{\chi}_4^0$ (‘Z2Z4’), $\tilde{\chi}_2^0\tilde{\chi}_3^0$ (‘Z2Z3’), $\tilde{\chi}_2^0\tilde{\chi}_2^0$ (‘Z2Z2’), some other neutralino pair (‘Other’), or other events ‘Bad’.

while those due to $\tilde{\chi}_2^0\tilde{\chi}_3^0$ events are enclosed in the legs of the short wedge terminating at $\sim 80\text{ GeV}$. Events from $\tilde{\chi}_2^0\tilde{\chi}_4^0$ decays span both of these regions and beyond up to the final kinematic edge¹⁰ at $\sim 200\text{ GeV}$.

Fig. 3(b,c) is color-coded to show the separate distributions of events from different production channels (A, H, or ‘direct’ production \equiv DP) and by their assorted neutralino-pair types; these distributions agree with remarks in the previous paragraph. Note, however, the presence of ‘bad’ events which do not distribute themselves nicely within the kinematic bounds and which are typically due to chargino decays. Though nearly 10 percent of the total number of events are bad events, about half of these are excluded by rejecting events outside the overall wedge structure, nicely illustrating the strength of the wedgebox technique.

Without the assistance of the wedgebox plot, one might be led to assume that events with $M_{e^+e^-} < 60\text{ GeV}$ correspond mostly to the decay topology of (2.1) with $i = j = 2$. This, however, leads to a Higgs boson mass distribution as shown in Fig. 4a. There is neither a clear peak nor any kind of distinguishing feature near the correct value of $M_A = 600\text{ GeV}$. Evidently, what might seem the natural choice of using events from the densest region of the wedgebox plot is not optimal.

Instead, events should be selected from the most *homogeneous* zone of the wedgebox plot, which in this case consists of the outermost legs from 80 GeV to 200 GeV , corresponding mostly $A^0 \rightarrow \tilde{\chi}_2^0\tilde{\chi}_4^0$ (even without looking at Fig. 4b, [33] predicts that events in the outer wedge of a double-wedge plot come from Higgs boson decays). As seen in Fig. 4b, the N-MST method now works splendidly, yielding an easily-identified peak at the correct Higgs boson mass, even though now an additional sparticle mass plays into the equations. The goodness of fit is more surprising considering the number of ‘bad’ events distributed throughout this zone; inspection reveals that these latter, however, often fail

¹⁰In the MSSM there are other possibilities for these edges aside from those of the form $\tilde{\chi}_j^0 \rightarrow l^+l^-\tilde{\chi}_1^0$, including $\tilde{\chi}_j^0 \rightarrow l^+l^-\tilde{\chi}_2^0$ and $\tilde{\chi}_2^\pm \rightarrow l^+l^-\tilde{\chi}_1^\pm$. Separate studies of decay kinematics can potentially exclude such possibilities. For parameter set choices examined herein, these other feasible decay modes have a totally negligible effect.

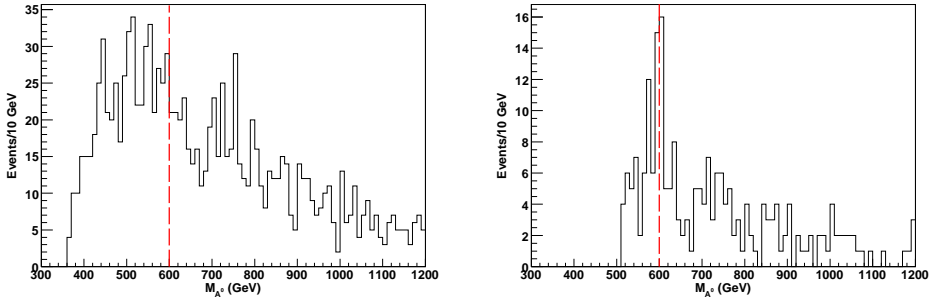


Figure 4. (a) Distribution of solutions for events taken from the inner box region of Fig. 3a; i.e., within the first set of dotted lines at ~ 60 GeV. Here the correct Higgs boson mass of $M_A \approx 600$ GeV does not appear at the peak. (b) Distribution of solutions for events taken from the outer legs of Fig. 3a; i.e., within the regions bounded by dotted lines at ~ 80 GeV and ~ 200 GeV. Here the correct Higgs boson mass of $M_A \approx 600$ GeV coincides with the peak.

to give solutions to equations (2.2)-(2.9), so they do not heavily interfere with the shape of the distribution.

Improvement of the N-MST method via a wedgebox plot, at least for the Higgs boson decay topology considered here, is therefore quite straightforward.

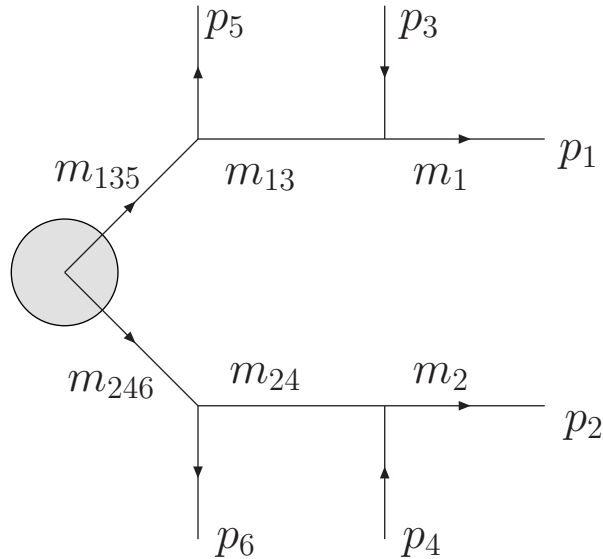


Figure 5. Event topology, taken from [28–30].

3 The C-MST Method of Cheng *et al.*

Next consider the C-MST method. The process treated by Cheng *et al.* [28–30] is illustrated in Fig. 5 in which the masses m_1 , m_2 , m_{13} , m_{24} , m_{135} and m_{246} must satisfy a set of

equations precisely analogous to (2.2)-(2.9):

$$m_1^2 = p_1^2 \quad (3.1)$$

$$m_2^2 = p_2^2 \quad (3.2)$$

$$m_{13}^2 = (p_1 + p_3)^2 \quad (3.3)$$

$$m_{24}^2 = (p_2 + p_4)^2 \quad (3.4)$$

$$m_{135}^2 = (p_1 + p_3 + p_5)^2 \quad (3.5)$$

$$m_{246}^2 = (p_2 + p_4 + p_6)^2 \quad (3.6)$$

$$p_{\text{sum}}^x = \sum_i p_i^x \quad (3.7)$$

$$p_{\text{sum}}^y = \sum_i p_i^y \quad (3.8)$$

where the transverse momentum sums $p_{\text{sum}}^{x,y}$ are assumed to be calculable from measurements of associated jet momenta (produced, though not shown, in the gray bubble in Fig. 5) and missing momentum (from the LSPs) necessary to balance the whole:

$$p_{\text{sum}}^x = \sum_l p_l^x + p_{\text{miss}}^x \quad p_{\text{sum}}^y = \sum_l p_l^y + p_{\text{miss}}^y \quad (3.9)$$

The specific example considered in [28–30] was production of two neutralinos via squarks in the MSSM, followed by decay via on-shell smuons to muons and two LSPs:

$$\tilde{q}\tilde{q} \rightarrow q q \tilde{\chi}_2^0 \tilde{\chi}_2^0 (\rightarrow \tilde{\mu}^\pm \mu^\mp \rightarrow \mu^+ \mu^- \tilde{\chi}_1^0) \quad (3.10)$$

giving

$$\begin{aligned} m_1 &= m_2 = m_{\tilde{\chi}_1^0} \\ m_{13} &= m_{24} = m_{\tilde{\mu}} \\ m_{135} &= m_{246} = m_{\tilde{\chi}_2^0} \end{aligned} \quad (3.11)$$

In the three-dimensional space of masses $(m_{\tilde{\chi}_1^0}, m_{\tilde{\chi}_2^0}, m_{\tilde{\mu}})$, each event gives eight equations (3.1)-(3.8) for the eight unknown LSP momenta p_1^μ and p_2^μ , assuming the outgoing muon momenta p_3, p_4, p_5, p_6 can be measured. The solution to this set of equations is again, as for the system of (2.2)-(2.9), a quartic equation with 0, 2, or 4 real roots. In contrast to the discussion of the last section, however, rather than trying to find the point in $(m_{\tilde{\chi}_1^0}, m_{\tilde{\chi}_2^0}, m_{\tilde{\mu}})$ -space where the density of solutions ($\equiv \mathbb{N}(m_{\tilde{\chi}_1^0}, m_{\tilde{\chi}_2^0}, m_{\tilde{\mu}})$) is maximized, instead the point where the *gradient* of \mathbb{N} is maximized (a heuristic argument for this is given in [28–30]) is sought.

In [28–30] this method apparently works quite well at the MSSM parameter points studied, giving all relevant sparticle masses to a few percent after collection of data samples corresponding to 300 fb^{-1} of integrated LHC luminosity. However, to test the robustness of this technique and the extent to which augmentation with the wedgebox technique can improve results, consider a new MSSM parameter point (see Tab. 1 again for masses):

MSSM Test Point II

$$\begin{aligned}
\mu &= -150 \text{ GeV} & M_2 &= 250 \text{ GeV} & M_1 &= 90 \text{ GeV} \\
\tan \beta &= 5 & M_{\widetilde{e}, \widetilde{\mu}_L, \widetilde{\tau}} &= 250 \text{ GeV} & M_{\widetilde{e}, \widetilde{\mu}_R} &= 120 \text{ GeV} \\
M_A &= 700 \text{ GeV} & M_{\widetilde{q}} &= 400 \text{ GeV} & M_{\widetilde{g}} &= 500 \text{ GeV}
\end{aligned}$$

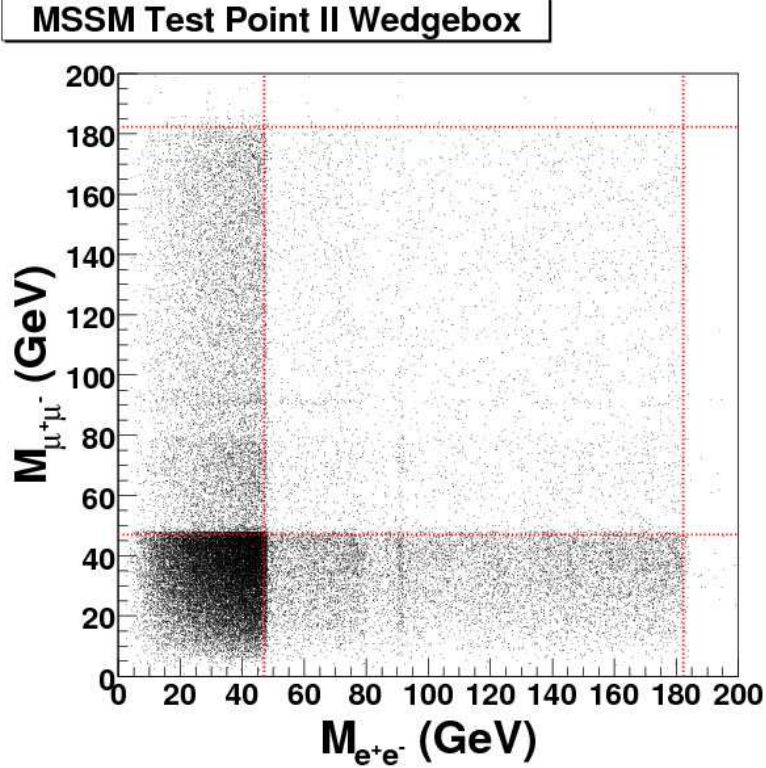


Figure 6. *Wedgebox at MSSM Test Point II for a luminosity of 90 fb^{-1} .*

3.1 Wedgebox selection

The wedgebox structure¹¹ of Fig. 6 is again generated using ISAJET [39, 40] and the event selection criteria mentioned earlier (save no jet cut); the plot compartmentalized into four substantially event-populated regions by the shown red-dashed lines to which will be applied the following nomenclature:

The Zone 1 box, with $[M_{ee} \text{ and } M_{\mu\mu}] < 47 \text{ GeV}$, is the most densely-populated region of the wedgebox plot and should include all $\widetilde{\chi}_2^0 \widetilde{\chi}_2^0$ events.

Zone 2 is composed of two rectangles (the legs of wedges) running outwards along both axes from the Zone 1 box — satisfying the condition that $[M_{ee} \text{ and } M_{\mu\mu}] < 182 \text{ GeV}$ and

¹¹ **MSSM Test Point II** is clearly representative of the general case in the MSSM, where pp collisions yield a ‘mixed bag’ of concomitant neutralino decays. Events on this plot pass the same cuts as in Section 2.1, minus the jet cut.

$[M_{ee} \text{ or } M_{\mu\mu} \text{ but not both}] < 47 \text{ GeV}$. Events due to $\tilde{\chi}_2^0 \tilde{\chi}_3^0$ and $\tilde{\chi}_2^0 \tilde{\chi}_4^0$ not residing in Zone 1 will fall¹² in Zone 2.

Zone 3, with $47 \text{ GeV} < [M_{ee} \text{ and } M_{\mu\mu}] < 182 \text{ GeV}$, lies outside of Zones 1 & 2 and should only be populated by $\tilde{\chi}_3^0 \tilde{\chi}_3^0$, $\tilde{\chi}_3^0 \tilde{\chi}_4^0$ and $\tilde{\chi}_4^0 \tilde{\chi}_4^0$ events.

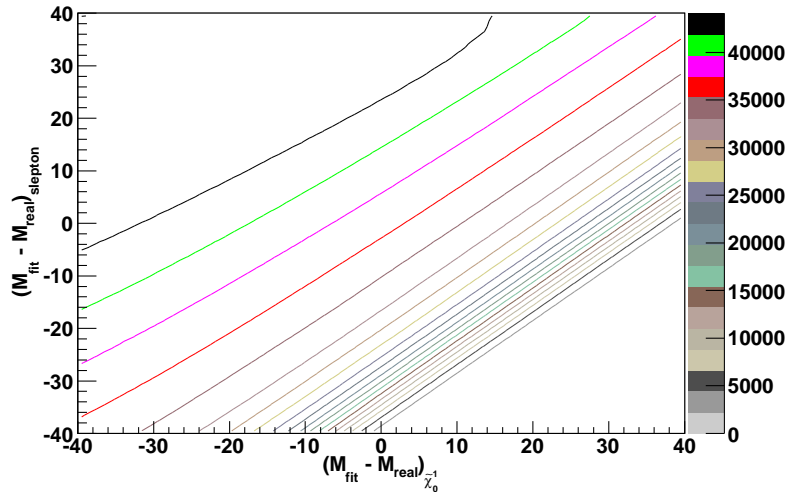


Figure 7. Mass space scan for MSSM Test Point II, using the whole sample from the wedgebox plot. The axes are the difference between the input mass and the real mass of LSP and slepton.

Consider first using four-lepton events across the whole wedgebox plot — this would include several different kinds of neutralino pair events. A scan was performed over the $(m_{\tilde{\chi}_1^0}, m_{\tilde{\chi}_2^0}, m_{\tilde{\mu}})$ mass space, and the resulting values projected onto the $(m_{\tilde{\chi}_1^0}, m_{\tilde{\mu}})$ -plane. As Table 1 shows $m_{\tilde{\mu}} - m_{\tilde{\chi}_1^0} \sim 41 \text{ GeV}$, Fig. 7 indicates that the gradient of \bar{N} maximizes along the line $m_{\tilde{\chi}_1^0} = m_{\tilde{\mu}}$ rather than at the desired true value: the C-MST method fails *badly* in this attempt to find the sparticle masses. Since the wedgebox plot clearly indicates that $\tilde{\chi}_2^0 \tilde{\chi}_3^0$, $\tilde{\chi}_2^0 \tilde{\chi}_4^0$ and $\tilde{\chi}_4^0 \tilde{\chi}_4^0$ production is substantial, the failure of the C-MST is not surprising given the inhomogeneity of the data set.

Consider instead performing an analysis limited to events in Zone 3 — which should be more homogeneous. Before proceeding though one more feature of the wedgebox plot should be taken into account: there is a clear Z -line at $[M_{ee} \text{ or } M_{\mu\mu}] \simeq 91 \text{ GeV}$. This is due to neutralinos decaying to an LSP and a pair of leptons via an on-shell Z^0 rather than via a slepton¹³. The situation is greatly simplified if the events in Zone 3 are further curtailed to encompass only those for which $100 \text{ GeV} < [M_{ee} \text{ and } M_{\mu\mu}] < 182 \text{ GeV}$. This truncated Zone 3 will be called Zone 3'. This will exclude the on-shell Z^0 events along with those due to $\tilde{\chi}_3^0 \tilde{\chi}_3^0$ or $\tilde{\chi}_3^0 \tilde{\chi}_4^0$. The remaining fairly homogeneous subset of events still yields 1000+ signal events (corresponding to 90 fb^{-1} of LHC integrated luminosity), 80% of which are

¹²With the $\tilde{\chi}_2^0 \tilde{\chi}_3^0$ ($\tilde{\chi}_2^0 \tilde{\chi}_4^0$) events terminating at M_{ee} or $M_{\mu\mu} \simeq 80 \text{ GeV}$ (182 GeV). The endlines at $\simeq 80 \text{ GeV}$ are faintly discernible in Fig. 6; however, the forthcoming analysis does not rely upon this.

¹³Although the missing energy cut should eliminate most SM $Z^0 Z^0$, $Z^0 Z^{0*}$ events, any such remnant background surviving would also populate this line.

in fact due to $\tilde{\chi}_4^0 \tilde{\chi}_4^0$ pair production (the remainder mostly involve colored sparticle decays into the heavier chargino, $\tilde{\chi}_2^\pm$).

Additional improvements in the results are possible if another piece of information is utilized: the numerical value¹⁴ for the edge of the $\tilde{\chi}_4^0 \tilde{\chi}_4^0$ box, Δ . It is clear that this edge can be measured quite accurately via the wedgebox or the traditional one-dimensional triangular mass distribution, yielding a relation between the three masses in the equation:

$$\Delta = m_{\tilde{\chi}_4^0} \sqrt{1 - \frac{m_{\tilde{\mu}}^2}{m_{\tilde{\chi}_4^0}^2}} \sqrt{1 - \frac{m_{\tilde{\chi}_1^0}^2}{m_{\tilde{\mu}}^2}} . \quad (3.12)$$

This additional information enables one to scan for only $m_{\tilde{\chi}_1^0}$ and $m_{\tilde{\mu}}$, with the $\tilde{\chi}_4^0$ mass calculated by solving the equation above.

Proceeding somewhat gradually, first consider applying an analysis incorporating Δ to the neutralino events from Zone 3', but with no detector effects and with the simulation co-opted to only include correct lepton placements in Fig. 5. The result, shown in Fig. 8, indicates that the desired physical mass is indeed given quite accurately by the point of steepest descent for \mathbb{N} .

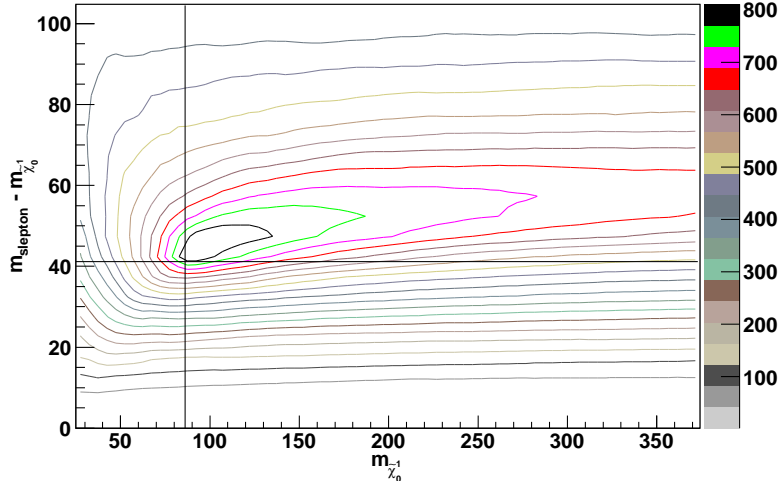


Figure 8. Two-dimensional scan result using events from Zone 3' without detector effects and with correct lepton placements. The horizontal axis is the $\tilde{\chi}_1^0$ mass, and the vertical axis is the mass difference of slepton and $\tilde{\chi}_1^0$. The horizontal and vertical lines show the correct values for $m_{\tilde{\mu}} - m_{\tilde{\chi}_1^0}$ and $m_{\tilde{\chi}_1^0}$, respectively.

Continuing on to the more realistic Zone 3' analysis including detector smearing and possible lepton placement errors leads to the result shown in Fig. 9. Clearly results are

¹⁴It is acknowledged that this runs counter to the statement in the introductory remarks that the edge locations are used purely to delineate the data set and not to provide additional numerical information. However, it would be foolish to completely ignore this extra information that is readily accessible. The aim herein is to emphasize how the wedgebox can be used to purify a data set, not to exclude the use of additional useful information.

worse than in Fig. 8, but the point of the steepest descent of N is still close to the physical mass.

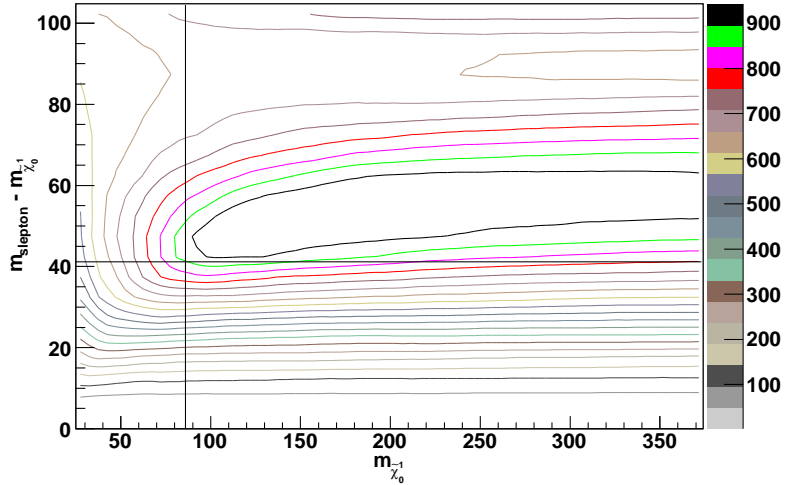


Figure 9. Two-dimensional scan result using 1080 events from Zone 3', incorporating detector effects and excluding simulation information not available to the experimentalists concerning correct lepton placement.

One reason for persisting inaccuracy is difficulty in applying the momentum conservation relation (3.9) — primarily due to detector smearing affects. With a simulation, one is able to compare the ('parton level') net transverse momentum of the two neutralinos produced by the generator (prior to their decay), labeled as p_{parton} , to the sum of the momenta of the four leptons in the signal plus the missing momentum, designated as p_{calc} . If p_{parton} and p_{cal} actually match the quantities on the left- and right-hand sides of Eqns. (3.9), respectively, then they should be equal. However, as illustrated by Fig. 10, this is not the case. The difference arises from the detector smearing¹⁵ of the lepton momenta (in addition the smearing of the momenta of the other observed particles alters the value calculated for the missing momentum¹⁶). The range of the imbalance between the experimentally-measurable value of p_{calc} and the desired value of p_{parton} is $-30 \text{ GeV} \gtrsim p_T \gtrsim 30 \text{ GeV}$. This is formidable in light of the fact that a small inaccuracy in p_T (say 2 GeV) can change the number of solutions at a given mass point by 10%. If smearing effects could be eliminated, so that p_{calc} would essentially be equal to p_{parton} , fits to masses would be quite good (easily

¹⁵Particle resolutions, adopted to approximate the CMS detector, are given by $\frac{\Delta p_i}{p_i} \propto \sqrt{r_1^2/p_i + r_2^2}$ where $r_1(r_2) = 0.8(0.03)$ for muons or hadrons with $|\eta| < 2.6$, $1.0(0.05)$ for muons or hadrons with $2.6 \leq |\eta| < 4.0$; and $r_1(r_2) = 0.03(0.005)$ for electrons and photons with $|\eta| < 4.0$.

¹⁶Another possible source of error is if the missing momentum is not solely due to the two LSP's produced in the neutralino decays. There could also be SM neutrinos produced in some events. With cascade production, the initial gluinos or squarks will lead to quark jets with significant p_T in addition to the desired neutralino pair. Decays of heavy-flavored quarks within these quark jets may well yield such neutrinos, especially if heavy-flavored sparticle production or decays of gluinos into heavy-flavored quarks is enhanced, as is expected in some scenarios [42]. How such neutrinos might affect a CMST-style analysis is currently under investigation [43].

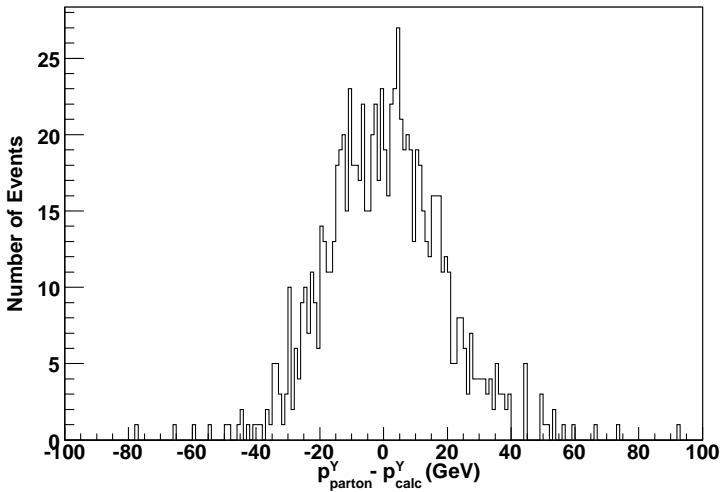


Figure 10. p_T distribution for one of the transverse directions. Here p_{parton} designated the net momentum of the two neutralinos (prior to their decay) while p_{calc} is the sum of the four leptons' momenta plus the calculated missing momentum. Thus p_{calc} includes detector smearing effects.

within 1%). Unfortunately, actual experiments cannot know how large the p_T imbalance between p_{parton} and p_{calc} is in any given event: the best that can be done is to perform a scan over this p_T uncertainty for each event, taking for instance $-10 \text{ GeV} < p_T < 10 \text{ GeV}$. This is done in making Fig. 11, whose maximum does lie somewhat closer to the actual LSP mass; however, since the correct value of $m_{\tilde{\mu}} - m_{\tilde{\chi}_1^0}$ was assumed in this 1-D projection, the result is somewhat better than what would be obtained in practice. The fitted LSP mass in Fig. 11 has a small error but with a slightly up-biased central value (primarily due to the fact that the neutralino pairs do not have a fixed CM energy).

4 Discussion & Conclusions

Use of a wedgebox plot to select the most homogeneous sample of events has been shown to increase the accuracy and efficacy of the N-MST and C-MST mass reconstruction methods. If the events analyzed do not mostly share the same decay topology, both methods fail. A wedgebox analysis can ascertain whether or not this is the case. If the wedgebox is a simple box, then a mass reconstruction analysis can proceed with confidence¹⁷. However, over much of the allowable MSSM parameter space the topology of the wedgebox plot is not merely a lone box — if a wedge or composite structure is observed, then selecting events from the legs of the wedge or the outer areas generally proves the most effective. Note that this runs counter to the choices made in all the N-MST and C-MST publications. In [31] for instance, some care is taken to describe the desirability of so-called ‘symmetric events’ — where both legs from the original parent particle contain the same intermediate

¹⁷It is true that at the Snowmass Benchmark point SPS1a [34], a simple box does describe the wedgebox topology of a few processes studied *at this point*. But these SPS1a studies [11–16, 24, 26] are certainly not representative of many other perfectly allowable parameter set choices and/or signature selections.

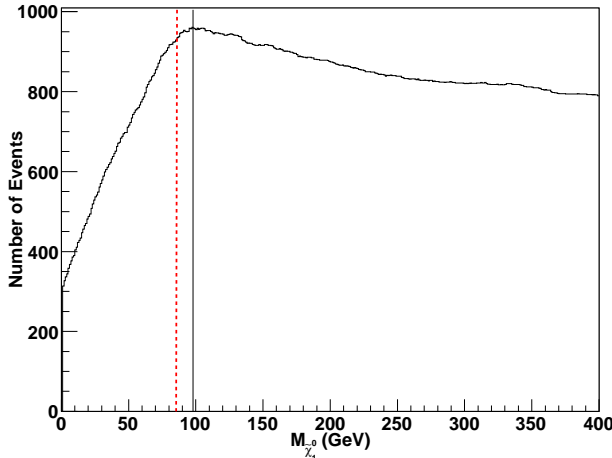


Figure 11. 1-D projection of Fig. 9, assuming the correct value of $m_{\tilde{\mu}} - m_{\tilde{\chi}_1^0}$, and scanning over $-10 \text{ GeV} < p_T < 10 \text{ GeV}$. The maximum of the curve, $m_{\tilde{\chi}_1^0} = 98 \pm 5 \text{ GeV}$, roughly approximates the actual LSP mass (86 GeV), given by the red dashed line.

particle states. The present work, on the other hand, makes the case that the benefits from using un-symmetric decay legs, e.g. efficient isolation of events with the same decay chain structure, may well trump the convenience of symmetric events in the subsequent MST analysis, and therefore unsymmetric events should not be ignored or viewed as an unnecessary complication.

Note that the time scale required to collect a sufficient number of events to generate a wedgebox diagram is roughly comparable to that needed to perform an MST analysis. This is in spite of the fact that the wedgebox technique rely upon populating scatter plots while an MST analysis *in principle* only requires collection of enough events to simultaneously solve the requisite equations. *In practice*, ambiguity in assigning the leptons and multiple solutions to the resulting quartic equation (see bulleted items in Secn. 2) as well as experimental factors (also enumerated earlier) necessitate a far larger sample of events to perform either of the MST analyses discussed. Further, and even more compellingly, without augmentation by the wedgebox technique¹⁸, applying an MST analysis to a quite limited data set is tantamount to wild speculation as to what SUSY channels are actually present and the results of such an analysis must be viewed most cautiously.

Scanning over the CM p_T in a $\pm 10 \text{ GeV}$ -window can also enhance the data analysis. Assumptions that the partonic CM has no transverse momentum (as implied by equations (2.9) and (3.9)) are basically incorrect; while in the N-MST method this does not seem to matter, the C-MST method is much more sensitive to this parameter. An ‘averaging’

¹⁸ And/or some other methodology yielding comparable information. The wedgebox technique does offer easily interpretable results, and the di-particle invariant mass distributions the technique relies upon cluster near the endpoints, *i.e.*, they have triangular distributions, which aid in obtaining clear results. The authors are unaware of other proposed techniques specifically designed for ascertaining which MSSM production and decay modes are represented in an experimental data set culled by excluded SM event types.

over p_T improves the result, but perhaps a more detailed analysis should eventually be performed as the latest set of structure functions and other knowledge of QCD becomes available.

The MST analyses presented here also assume that the decay chain involved is a series of two-body decays via intermediate on-mass-shell sleptons. This need not be the case, and the on-mass-shell assumption should be tested. This however is beyond the purview of the wedgebox technique. The di-lepton distribution shapes for on- and off-shell decays are not identical [10, 32], and this could be used to distinguish between the two possibilities; however, the effects of cuts, backgrounds and a finite-sized data set must be considered. Ref. [44] notes that distribution shapes for on-shell (sequential two-body decays) and off-shell (three-body decays) are effectively indistinguishable for some parameter choices. Also, Ref. [45] finds that the shape of the di-lepton distribution may be affected by the nature of the neutralinos (the extent to which they are gauginos or higgsinos), illustrating how dynamical issues arising from the nature of the coupling involved in a decay may not be separable from purely kinematic issues associated with the relevant masses.

So an alternative to a straight-forward examination of the di-lepton distribution shape is desirable [20]. The Decay Kinematics (DK) technique [46–48] might offer such an alternative wherein cross-correlating different invariant mass distributions resolves the on-shell *vs.* off-shell issue. Another idea was put forward in [49]¹⁹, wherein a rudimentary sketch of a very Dalitz-esque technique to look for the presence of two-body decay chains is presented — a realistic study applying this idea would be interesting. Refs. [20, 50] instead champion a ‘Markov chain’ approach to analyzing the event sample where “no assumption is made about the processes causing the observed endpoints.” Supposedly then the issue of whether the sleptons are on-mass-shell or off-mass-shell is rendered moot to the more modest goal of determining a region of parameter space consistent with the data in a non-MST analysis²⁰.

The present work may be thought of as an early installment of a much grander programme to fuse all known kinematic mass reconstruction methods together. The make-up of this programme consists not only of combining fits from different methods for a static event sample set, but also of improving the composition of the event set under consideration, as symbolically-depicted in Fig. 12. In the present work where the wedgebox technique is used to select (to the degree possible) events due to a *specific* $\tilde{\chi}_i^0 \tilde{\chi}_j^0$ neutralino pair²¹ Once a fairly homogeneous event sample is obtained²² then it becomes straightforward to apply various mass reconstruction methods and cross-check them. For example, in the case of Higgs boson decay considered here, one could try matching the N-MST results presented here to those from a study of 4-lepton invariant mass endpoints [41] — it would be especially instructive to compare results at the SPS1a parameter point, for example, where both techniques, in the total ignorance of sparticle masses, give poor results individually,

¹⁹See pages 50–51 therein.

²⁰Though suggested, this issue is not explored in any detail in either of these works.

²¹Situations in which $m_{\tilde{e}} \neq m_{\tilde{\mu}}$ may also be amenable to such analyses.

²²An alternative track is attempted in Ref. [50], wherein the idea is to deal with all of the complexity of a mixed data set in the mass analysis program, rather than bifurcate the analysis into a purifying stage and then an analysis stage. The inherent weakness of this approach is that results from studying just the simplest subset of the events are impeded by the need to disentangle more confusing events.

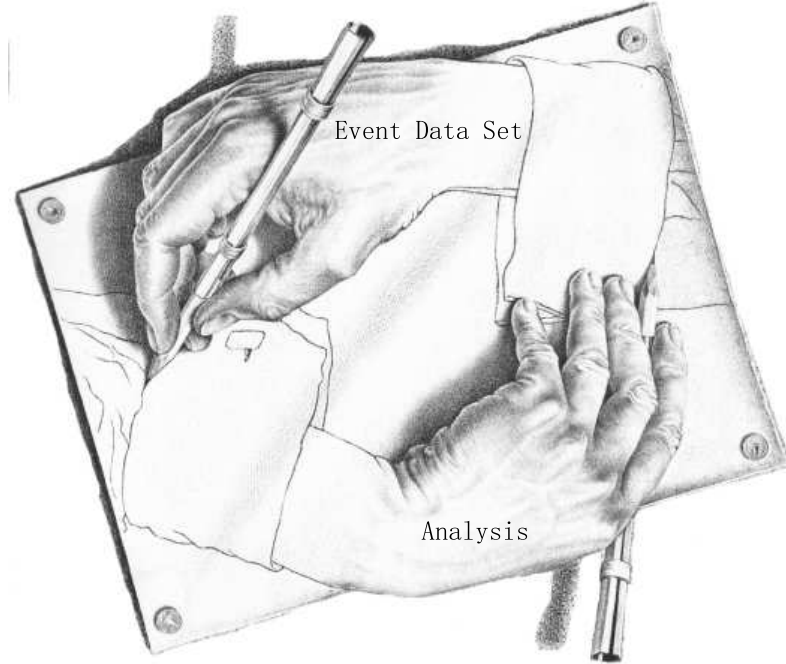


Figure 12. This famous lithograph by M.C. Escher is adapted to emphasize the symbiosis between the analysis and the data set — the latter is best not seen as static from the onset of the former.

but may give a stronger result in unison[51].

An MST analysis is then an attractive option if enough mass-shell conditions can be found to match the number of mass components of the invisible final-state particles, as is the case for the LSP-generating SUSY decay chains considered herein. Further though, the present work shows how endpoint information funneled through the wedgebox technique can positively supplement such an MST analysis, as in the augmented C-MST study presented in Secn. 3. No mass-reconstruction technique is immune from possessing potentially faulty assumptions, and so coupling several complementary analysis techniques will in general improve reliability as well as accuracy²³.

Likewise, consideration of suitable inclusive variables, such as the m_{T2} variable[52–54] and its variants [55, 56], to augment either an MST study [31] or an endpoint analysis [21–24, 57–62] has been shown to be beneficial, at least in some cases. Then there is the entire array of *dynamical* (and thus model-dependent) information associated with cross-sections and the shapes(spread) of events plotted against one(or more) parameters. As noted earlier, kinematics can never really be totally divorced from the present dynamics. MSSM/mSUGRA studies combining information from cross-sections [50] or distribution shapes [62–64] with that from an endpoint analysis have also been performed and are no doubt the vanguard of many more such studies, at least if initial LHC results prove favorable. And, when those first major blocks of data from the LHC become available,

²³Also minimizing overlapping information content between the analysis components will increase efficiency. Whether or not this is a significant issue would depend on how cpu-intensive the techniques are and on the computing resources available.

application of numerous analysis techniques — including the wedgebox techniques, would be a good idea.

5 Acknowledgements

This work was supported in part by the National Natural Science Foundation of China Grant No. 10875063 to MB and RL.

References

- [1] *ATLAS detector and physics performance. Technical design report. Vol. 2*, . CERN-LHCC-99-15.
- [2] CMS Collaboration, G. L. Bayatian *et. al.*, *CMS technical design report, volume II: Physics performance*, *J. Phys.* **G34** (2007) 995–1579.
- [3] B. C. Allanach *et. al.*, *Measuring supersymmetric particle masses at the LHC in scenarios with baryon-number R-parity violating couplings*, *JHEP* **03** (2001) 048, [[hep-ph/0102173](#)].
- [4] F. E. Paige, *Determining SUSY particle masses at LHC*, [hep-ph/9609373](#).
- [5] I. Hinchliffe, F. E. Paige, M. D. Shapiro, J. Soderqvist, and W. Yao, *Precision SUSY measurements at CERN LHC*, *Phys. Rev.* **D55** (1997) 5520–5540, [[hep-ph/9610544](#)].
- [6] F. Gianotti, *Precision SUSY measurements with ATLAS: SUGRA "Point 4"*, Tech. Rep. ATL-PHYS-97-110. ATL-GE-PN-110, CERN, Geneva, Sep, 1997.
- [7] I. Hinchliffe and F. E. Paige, *Measurements in gauge mediated SUSY breaking models at LHC*, *Phys. Rev.* **D60** (1999) 095002, [[hep-ph/9812233](#)].
- [8] I. Hinchliffe and F. E. Paige, *Measurements in SUGRA models with large tan(beta) at LHC*, *Phys. Rev.* **D61** (2000) 095011, [[hep-ph/9907519](#)].
- [9] B. Mura and L. Feld, *Determination of Neutralino Masses with the CMS Experiment*. *oai:cds.cern.ch:1311179*. PhD thesis, Aachen, Tech. Hochsch., Aachen, 2006. Presented on Dec 2006.
- [10] H. Bachacou, I. Hinchliffe, and F. E. Paige, *Measurements of masses in SUGRA models at CERN LHC*, *Phys. Rev.* **D62** (2000) 015009, [[hep-ph/9907518](#)].
- [11] B. K. Gjelsten, D. J. Miller, 2, and P. Osland, *Measurement of SUSY masses via cascade decays for SPS 1a*, *JHEP* **12** (2004) 003, [[hep-ph/0410303](#)].
- [12] B. K. Gjelsten, D. J. Miller, 2, and P. Osland, *Measurement of the gluino mass via cascade decays for SPS 1a*, *JHEP* **06** (2005) 015, [[hep-ph/0501033](#)].
- [13] B. K. Gjelsten, D. J. Miller, 2, and P. Osland, *Resolving ambiguities in mass determinations at future colliders*, [hep-ph/0507232](#).
- [14] B. K. Gjelsten, D. J. Miller, 2, and P. Osland, *Determining masses of supersymmetric particles*, [hep-ph/0511008](#).
- [15] B. K. Gjelsten, E. Lytken, D. J. Miller, P. Osland, and G. Polesello, *A detailed analysis of the measurement of susy masses with the atlas detector at the lhc*, Tech. Rep. ATL-PHYS-2004-007, CERN, Geneva, Jan, 2004. Contribution to the proceedings : LHC/LC workshop.

- [16] B. K. Gjelsten, D. J. Miller, 2, P. Osland, and A. R. Raklev, *Mass ambiguities in cascade decays*, [hep-ph/0611080](#).
- [17] D. J. Miller, 2, P. Osland, and A. R. Raklev, *Invariant mass distributions in cascade decays*, *JHEP* **03** (2006) 034, [[hep-ph/0510356](#)].
- [18] E. Lytken, *Derivation of some kinematical formulas in susy decay chains*, Tech. Rep. ATL-PHYS-2005-003. ATL-COM-PHYS-2004-001, CERN, Geneva, 2004.
- [19] J. M. Butterworth, J. R. Ellis, and A. R. Raklev, *Reconstructing sparticle mass spectra using hadronic decays*, *JHEP* **05** (2007) 033, [[hep-ph/0702150](#)].
- [20] C. G. Lester, M. A. Parker, and M. J. White, 2, *Three body kinematic endpoints in SUSY models with non- universal Higgs masses*, *JHEP* **10** (2007) 051, [[hep-ph/0609298](#)].
- [21] B. C. Allanach, C. G. Lester, M. A. Parker, and B. R. Webber, *Measuring sparticle masses in non-universal string inspired models at the LHC*, *JHEP* **09** (2000) 004, [[hep-ph/0007009](#)].
- [22] D. R. Tovey, *Measurement of the neutralino mass*, *Czech. J. Phys.* **54** (2004) A175–A182.
- [23] I. Borjanovic, J. Krstic, and D. Popovic, *SUSY studies with Snowmass Point 5 mSUGRA parameters*, *Czech. J. Phys.* **55** (2005) B793–B799.
- [24] D. R. Tovey, *On measuring the masses of pair-produced semi-invisibly decaying particles at hadron colliders*, *JHEP* **04** (2008) 034, [[arXiv:0802.2879](#)].
- [25] R. Horsky, M. Kramer, 1, A. Muck, and P. M. Zerwas, *Squark Cascade Decays to Charginos/Neutralinos: Gluon Radiation*, *Phys. Rev.* **D78** (2008) 035004, [[arXiv:0803.2603](#)].
- [26] M. M. Nojiri, G. Polesello, and D. R. Tovey, *Proposal for a new reconstruction technique for SUSY processes at the LHC*, [hep-ph/0312317](#).
- [27] K. Kawagoe, M. M. Nojiri, and G. Polesello, *A new SUSY mass reconstruction method at the CERN LHC*, *Phys. Rev.* **D71** (2005) 035008, [[hep-ph/0410160](#)].
- [28] H.-C. Cheng, J. F. Gunion, Z. Han, G. Marandella, and B. McElrath, *Mass Determination in SUSY-like Events with Missing Energy*, *JHEP* **12** (2007) 076, [[arXiv:0707.0030](#)].
- [29] H.-C. Cheng, D. Engelhardt, J. F. Gunion, Z. Han, and B. McElrath, *Accurate Mass Determinations in Decay Chains with Missing Energy*, *Phys. Rev. Lett.* **100** (2008) 252001, [[arXiv:0802.4290](#)].
- [30] H.-C. Cheng, J. F. Gunion, Z. Han, and B. McElrath, *Accurate Mass Determinations in Decay Chains with Missing Energy: II*, *Phys. Rev.* **D80** (2009) 035020, [[arXiv:0905.1344](#)].
- [31] M. M. Nojiri, G. Polesello, and D. R. Tovey, *A hybrid method for determining SUSY particle masses at the LHC with fully identified cascade decays*, *JHEP* **05** (2008) 014, [[arXiv:0712.2718](#)].
- [32] M. Bisset *et. al.*, *Pair-produced heavy particle topologies: MSSM neutralino properties at the LHC from gluino / squark cascade decays*, *Eur. Phys. J.* **C45** (2006) 477–492, [[hep-ph/0501157](#)].
- [33] G. Bian, M. Bisset, N. Kersting, Y. Liu, and X. Wang, *Wedgebox analysis of four-lepton events from neutralino pair production at the LHC*, *Eur. Phys. J.* **C53** (2008) 429–446, [[hep-ph/0611316](#)].
- [34] B. C. Allanach *et. al.*, *The Snowmass points and slopes: Benchmarks for SUSY searches*, *Eur. Phys. J.* **C25** (2002) 113–123, [[hep-ph/0202233](#)].
- [35] G. Corcella *et. al.*, *HERWIG 6.5: an event generator for Hadron Emission Reactions With*

*Interfering Gluons (including supersymmetric processes), JHEP **01** (2001) 010, [[hep-ph/0011363](#)].*

[36] G. Corcella *et. al.*, *HERWIG 6.5 release note*, [hep-ph/0210213](#).

[37] S. Moretti, K. Odagiri, P. Richardson, M. H. Seymour, and B. R. Webber, *Implementation of supersymmetric processes in the HERWIG event generator*, JHEP **04** (2002) 028, [\[hep-ph/0204123\]](#).

[38] E. Richter-Was, D. Froidevaux, and L. Poggioli, *Atlfast 2.0 a fast simulation package for atlas*, Tech. Rep. ATL-PHYS-98-131, CERN, Geneva, Nov, 1998.

[39] H. Baer, F. E. Paige, S. D. Protopopescu, and X. Tata, *ISAJET 7.48: A Monte Carlo event generator for $p\ p$, $\text{anti-}p\ p$, and $e^+ e^-$ reactions*, [hep-ph/0001086](#).

[40] F. E. Paige, S. D. Protopopescu, H. Baer, and X. Tata, *ISAJET 7.69: A Monte Carlo event generator for $p\ p$, $\text{anti-}p\ p$, and $e^+ e^-$ reactions*, [hep-ph/0312045](#).

[41] P. Huang, N. Kersting, and H. H. Yang, *Model-Independent SUSY Masses from 4-Lepton Kinematic Invariants at the LHC*, Phys. Rev. **D77** (2008) 075011, [[arXiv:0801.0041](#)].

[42] R. H. K. Kadala, P. G. Mercadante, J. K. Mizukoshi, and X. Tata, *Heavy-flavour tagging and the supersymmetry reach of the CERN Large Hadron Collider*, Eur. Phys. J. **C56** (2008) 511–528, [[arXiv:0803.0001](#)].

[43] R. Lu and M. Bisset. Work in progress.

[44] S. Chouridou, R. Strhmer, and T. M. Trefzger, *Study of the three body matrix element of the neutralino decay 034*, Tech. Rep. ATL-PHYS-2003-034, CERN, Geneva, Jul, 2002.

[45] R. Kitano and Y. Nomura, *Supersymmetry, naturalness, and signatures at the LHC*, Phys. Rev. **D73** (2006) 095004, [[hep-ph/0602096](#)].

[46] N. Kersting, *A Simple Mass Reconstruction Technique for SUSY particles at the LHC*, Phys. Rev. **D79** (2009) 095018, [[arXiv:0901.2765](#)].

[47] Z. Kang, N. Kersting, S. Kraml, A. R. Raklev, and M. J. White, *Neutralino Reconstruction at the LHC from Decay-frame Kinematics*, Eur. Phys. J. **C70** (2010) 271–283, [[arXiv:0908.1550](#)].

[48] Z. Kang, N. Kersting, and M. White, *Mass Estimation without using MET in early LHC data*, [arXiv:1007.0382](#).

[49] M. E. Peskin, *Supersymmetry in Elementary Particle Physics*, [arXiv:0801.1928](#).

[50] C. G. Lester, M. A. Parker, and M. J. White, 2, *Determining SUSY model parameters and masses at the LHC using cross-sections, kinematic edges and other observables*, JHEP **01** (2006) 080, [[hep-ph/0508143](#)].

[51] N. Kersting. Work in progress.

[52] C. G. Lester and D. J. Summers, *Measuring masses of semiinvisibly decaying particles pair produced at hadron colliders*, Phys. Lett. **B463** (1999) 99–103, [[hep-ph/9906349](#)].

[53] A. Barr, C. Lester, and P. Stephens, *$m(T2) : The Truth behind the glamour$* , J. Phys. **G29** (2003) 2343–2363, [[hep-ph/0304226](#)].

[54] C. Lester and A. Barr, *MTGEN : Mass scale measurements in pair-production at colliders*, JHEP **12** (2007) 102, [[arXiv:0708.1028](#)].

[55] A. J. Barr, C. G. Lester, M. A. Parker, B. C. Allanach, and P. Richardson, *Discovering*

anomaly-mediated supersymmetry at the LHC, *JHEP* **03** (2003) 045, [[hep-ph/0208214](#)].

[56] M. Serna, *A short comparison between m_{T2} and m_{CT}* , *JHEP* **06** (2008) 004, [[arXiv:0804.3344](#)].

[57] M. M. Nojiri, Y. Shimizu, S. Okada, and K. Kawagoe, *Inclusive transverse mass analysis for squark and gluino mass determination*, *JHEP* **06** (2008) 035, [[arXiv:0802.2412](#)].

[58] W. S. Cho, K. Choi, Y. G. Kim, and C. B. Park, *Measuring superparticle masses at hadron collider using the transverse mass kink*, *JHEP* **02** (2008) 035, [[arXiv:0711.4526](#)].

[59] W. S. Cho, K. Choi, Y. G. Kim, and C. B. Park, *Gluino Stransverse Mass*, *Phys. Rev. Lett.* **100** (2008) 171801, [[arXiv:0709.0288](#)].

[60] B. Gripaios, *Transverse Observables and Mass Determination at Hadron Colliders*, *JHEP* **02** (2008) 053, [[arXiv:0709.2740](#)].

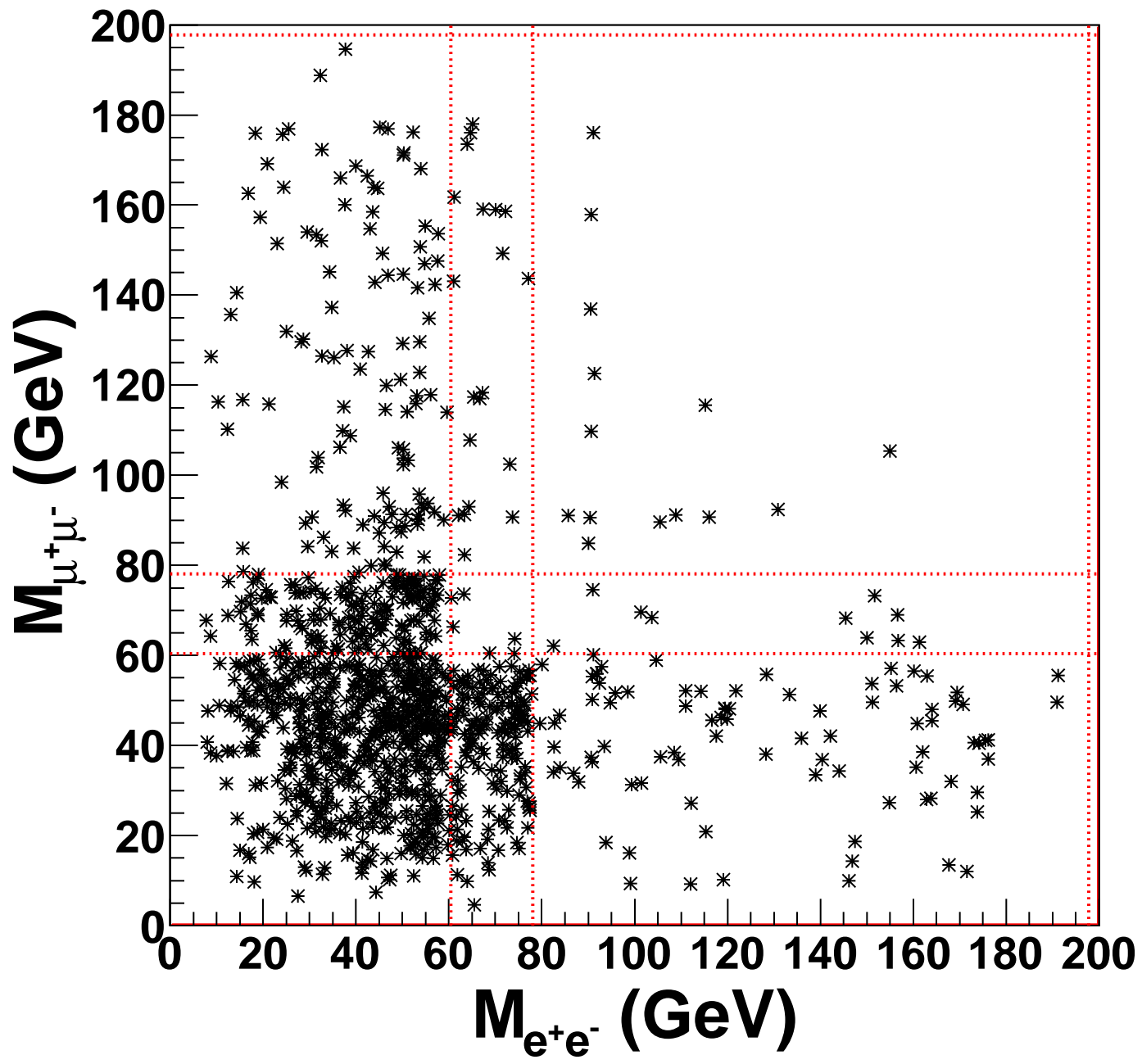
[61] A. J. Barr, B. Gripaios, and C. G. Lester, *Weighing Wimps with Kinks at Colliders: Invisible Particle Mass Measurements from Endpoints*, *JHEP* **02** (2008) 014, [[arXiv:0711.4008](#)].

[62] G. G. Ross and M. Serna, *Mass Determination of New States at Hadron Colliders*, *Phys. Lett.* **B665** (2008) 212–218, [[arXiv:0712.0943](#)].

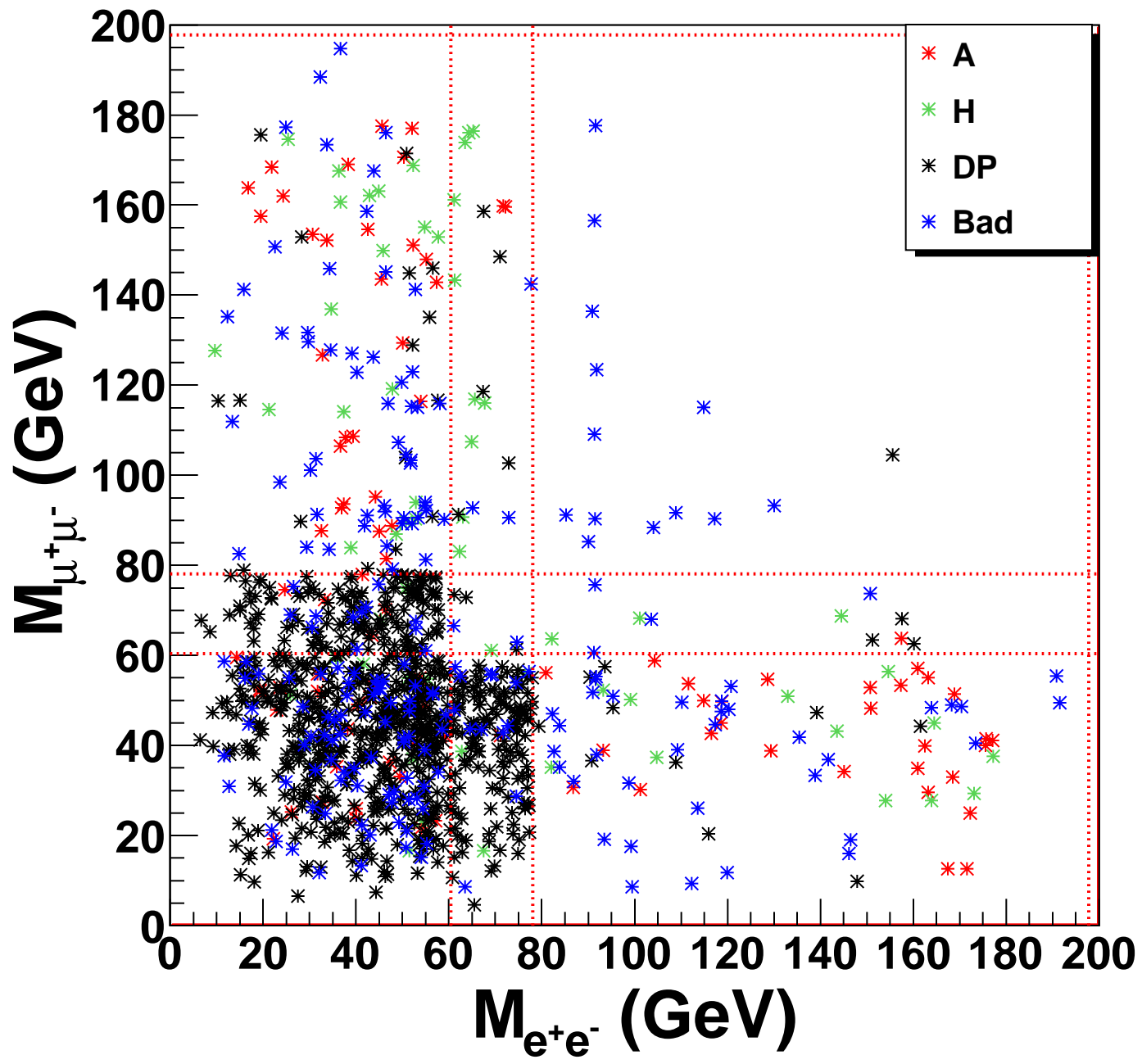
[63] B. K. Gjelsten, D. J. Miller, 2, P. Osland, and A. R. Raklev, *Mass Determination in Cascade Decays Using Shape Formulas*, *AIP Conf. Proc.* **903** (2007) 257–260, [[hep-ph/0611259](#)].

[64] C. G. Lester, *Constrained invariant mass distributions in cascade decays: The shape of the ' $m(qll)$ -threshold' and similar distributions*, *Phys. Lett.* **B655** (2007) 39–44, [[hep-ph/0603171](#)].

(a) Test Point I Wedgebox



(b) Test Point I Wedgebox



(c) Test Point I Wedgebox

